Genetic Algorithm-Based Approach for Mask Design Generation in Wet Etching Silicon Corrosion

Ana Paula Rehder[1], Marcos Sales Guerra Tsuzuki[2], Thiago de Castro Martins[3]

[1]University of Sao Paulo, anapaularehder@usp.br
[2]University of Sao Paulo, mtsuzuki@usp.br
[3]University of Sao Paulo, thiago@usp.br

Corresponding author: Ana Paula Rehder, anapaularehder@usp.br

Abstract. Anisotropic wet etching of silicon is pivotal in fabricating Microelectromechanical Systems (MEMS), leveraging silicon's crystallographic properties to create intricate microstructures. However, designing the appropriate photolithography mask to achieve a desired 3D structure through anisotropic etching poses a significant inverse problem because of the complex, direction-dependent etching rates of silicon's crystallographic planes. This paper introduces a novel method to solve this inverse problem by integrating a Genetic Algorithm (GA) with anisotropic etching simulations. The approach employs ViennaLS, an open-source level set library, to simulate the etching process, and OpenSCAD for 3D model manipulation and comparison. The desired device is discretized, and mask geometries are represented as binary arrays within the GA. The algorithm iteratively refines candidate mask solutions through selection, crossover, and mutation operations, aiming to minimize the volumetric difference between the etched structures and the target design. The simulation results validate the effectiveness of the proposed method in various test structures, including standard MEMS components such as beams and islands, as well as more complex devices such as optimized gyroscopes. The GA successfully identified mask geometries that produce the desired structures with a volumetric difference of less than 0.1% compared to the ideal device. An advanced feature of the algorithm is the automatic adjustment of the etching time based on the stabilization of fitness values, enhancing its ability to account for uncertainties in the etching behavior and process variations. This automated time optimization reduces the need for empirical trials, offering significant time and cost savings in MEMS design and fabrication. In conclusion, integrating genetic algorithms with anisotropic etching simulations presents a powerful tool for inverse mask design in MEMS fabrication. This innovative approach opens new avenues for efficient and cost-effective manufacturing of complex microstructures, addressing a critical challenge in the field of microfabrication.

Keywords: Microelectromechanical Systems (MEMS), Computational Simulations, Inverse Problem, Microfabrication, Mask Generation, Silicon Anisotropic Corrosion, Genetic algorithm
DOI: https://doi.org/10.14733/cadaps.2026.162-179

1 INTRODUCTION

Microelectromechanical systems (MEMS) are a key technology that enables the integration of mechanical and electrical components on a miniature scale [11]. These systems are widely used in a variety of applications, from sensors to actuators, combining microstructures, microsensors, microactuators, and microelectronics into a single silicon chip. The MEMS fabrication process typically involves complex steps such as photolithography, etching, and deposition, all of which are highly dependent on the properties of silicon, the most commonly used substrate in MEMS devices.

Silicon is favored because of its abundance, ease of processing, and high precision in shape reproduction through photolithography. Its ability to form an inert and insulating surface layer of silicon dioxide (SiO2) when oxidized further enhances its suitability for MEMS applications. Additionally, the anisotropic etching properties of silicon, which result in different etch rates along its crystallographic planes, allow for the formation of intricate 3D structures that are essential in MEMS design.

However, the fabrication of these microstructures is complex, and the precise control of the etching process is crucial to achieving the desired shapes. Recent advancements in modeling techniques, such as the Level Set method and Cellular Automata, have enabled better prediction and control of the etching behavior, especially in silicon-based MEMS devices. This paper investigates the use of optimization techniques, including Genetic Algorithms, to solve the inverse problem of mask design, where the goal is to determine the appropriate mask geometry that will yield a specific final structure after anisotropic silicon etching. This approach could significantly improve the efficiency and accuracy of MEMS fabrication processes.

The text has the following structure. Section 2 gives a detailed technical context. This paper describes MEMS, including the components, the role of silicon as a substrate, and why silicon is preferred for MEMS devices. Section 3 addresses the core research problem: how to generate mask geometries to produce specific structures through anisotropic etching. It is presented as an "inverse problem" and introduces optimization techniques, specifically using genetic algorithms. Section 4 outlines the simulations conducted to test the algorithm. The paper discusses the results for different structures (island and beam models), providing data on dimensions, discretization, and time to solution. Section 5 summarizes the findings, stating that the approach successfully produced the desired MEMS structures using anisotropic wet etching. Section 6 focuses on future improvements, such as integrating time as a parameter in the genetic algorithm and using finer discretization to tackle more complex devices such as accelerometers and gyroscopes.

2 BACKGROUND

Microelectromechanical Systems (MEMS) are a technological process used to create small devices or integrated systems that combine mechanical and electrical components [11]. In its most general form, MEMS consists of mechanical microstructures, microsensors, microactuators, and microelectronics, all integrated on the same silicon chip.

For the microfabrication of these devices, typically a substrate is used and a material is added to it, serving as an underlying layer to aid in the corrosion process. Following this layer, a photoresist film (light-sensitive material) is deposited to transfer the mask pattern in photolithography. Another process transfers the pattern from the photoresist layer to the underlying layer, and after this process, the photoresist is removed.

According to [11], the most widely used substrate in microelectronics is silicon due to the following reasons:

a) it is abundant, cheaper and can be processed with unparalleled purity;

b) thin film deposition on it is easy;

c) high-definition and reproduction of shapes using photolithography are perfect for high levels of MEMS precision;

d) silicon microelectronic circuits are batch-fabricated (a silicon wafer contains hundreds of identical chips, not just one);

e) it can be readily oxidized to form a chemically inert and electrically insulating surface layer of SiO_2 upon exposure to vapor.

Silicon also distinguishes itself from other materials because corrosion occurs at distinct rates in different crystallographic directions, known as anisotropic corrosion. According to [1], silicon belongs to the cubic diamond crystal structure.

During microfabrication, corrosion is a process that selectively removes materials, whether on the upper or lower surface of the wafer, using a mask pattern [6]. Silicon corrosion can be either dry or wet. Considering wet etching, in specific processes, anisotropic profiles result due to the high selectivity of the corrosion agent with the silicon's crystalline structure. This can lead to a multitude of shapes such as pyramidal cavities, V-shaped, hourglass-shaped, among others. When the vertically moving etch fronts from both sides meet, a sharp corner is formed. Then, lateral etching occurs, with fast etch planes such as 110 and 411 being exposed [6].

In this cases the concentration of the etchant critically influences the silicon etch rate, with two main strategies to achieve local maxima. Using diluted KOH (10 to 20 wt%) or TMAH (2 to 5 wt%) solutions offers ease of application but results in moderate etch rates and increased surface roughness due to micro-pyramid formation and, additionally, various additives such as redox systems and complexants have been explored to enhance etch rates, but their use remains uncommon due to limited further studies [10].

The resulting three-dimensional shapes are difficult to predict due to multiple dependencies, such as crystal orientation, composition, and temperature of the reagents, the use of additives, etc, as shown in Figure 1.

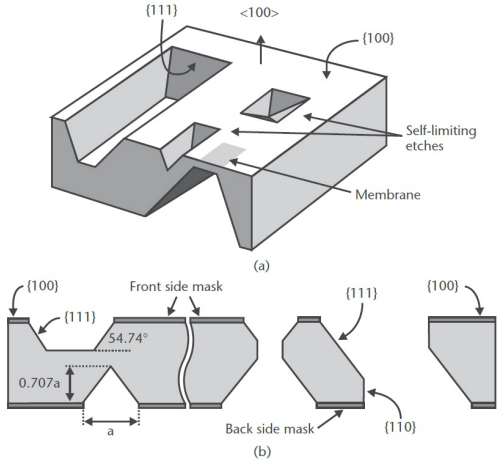

Figure 1: Silicon crystallographic planes wet corrosion [6].

Consequently, significant efforts have been made over the years to accurately model the process. Corrosion rates are generally given in the [100] direction, corresponding to the 100 crystallographic plane of silicon. The 110 plane is etched at a rate twice as high as the 100 plane, while the 111 plane is etched at a rate up to 100 times lower than the 100 plane [14].

To illustrate how the mask design can be non-trivial under anisotropic etching in silicon, let us consider a scenario where one aims to obtain a triangular beam. One might assume that by simply creating a triangular-shaped mask and performing the etching process, the desired structure could be achieved. However, the left side of Figure 2 illustrates that due to the crystalline structure of silicon, the entire structure begins to corrode, potentially even disappearing entirely. The ideal mask shape for this case would be the rectangular beam shown on the right. Through the etching of the silicon's crystalline structure, which varies in each direction within the crystal, it becomes possible to attain the desired final triangular structure.

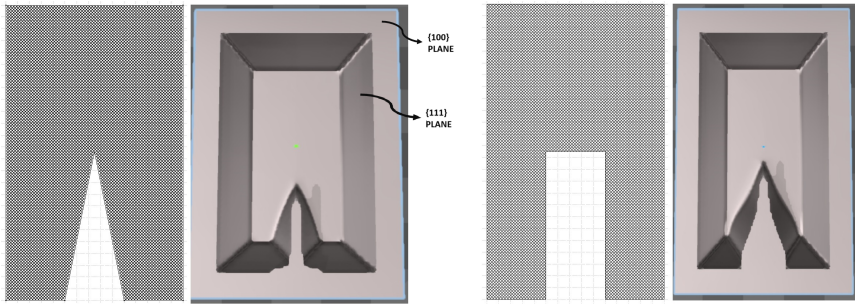

Figure 2: Triangular x rectangular beam mask.

Some techniques have been developed, such as Cellular Automata and Level Set methods, where there are essentially means to determine when an atom is removed from the surface and when it remains.

[12] described an application where etching rate anisotropy in silicon is modeled taking into account full silicon symmetry properties, by means of the interpolation technique using experimentally obtained values for the etching rates along thirteen principal and high index directions in KOH solutions. The resulting level set equations are solved using an open source implementation of the sparse field method (ITK library, developed in medical image processing community), extended for the case of non-convex Hamiltonians. According to them, Level set method, introduced by [8], is a powerful technique for analyzing and computing moving fronts in a variety of different settings. The angular dependence of the silicon corrosion rate is determined based on the symmetry properties of the silicon crystal.

The Sparse-Field method itself, developed by [17], uses an approximation to the level set function that makes it feasible to recompute the neighborhood of the zero level set at each time step. So, ViennaLS employs this approach in an open-source code to simulate anisotropic silicon corrosion, allowing users to define corrosion rates and time, as well as the mask to be used in the process.

Alongside ViennaLS and advancing to the stage of solving an inverse problem to obtain the mask leading to the desired device, the Genetic Algorithm comes into play. The Genetic Algorithm (GA) is a metaheuristic inspired by concepts from the theory of species evolution.

GA operates based on the principles of natural selection and survival of the fittest, established by Charles Darwin, as well as genetic elements such as chromosome crossover proposed by Gregor Mendel and mutation theory [7]. It can address various problems, including search and optimization. This metaheuristic was introduced by [5] and popularized by [4].

According to [7], in this algorithm, a set of potential solutions (initial population) is randomly generated within a search space. All possible solutions (individuals) in the population are evaluated using an objective function (fitness function), and a set of better-evaluated individuals (fittest) are selected. Then, the main

GA operations for generating offspring occur: Crossover, where genetic material exchange or mixing between parents takes place, and Mutation, where occasional changes in genetic material can occur, altering the individual. Through elitism, fitter individuals may be kept in the population while others are replaced by newly generated offspring, thus completing one generation.

In general, the number of generations required for convergence in a Genetic Algorithm (GA) is strongly influenced by the problem characteristics, including the complexity of the search space and the relative impact of decision variables on the fitness function. As demonstrated by recent studies, problems with smoother fitness landscapes tend to converge more rapidly, whereas problems with rugged or highly nonlinear search spaces typically require a significantly higher number of generations to reach satisfactory solutions [3].

3 METHODS

Mask geometry generation is considered an example of an Inverse Problem. Although the problem of determining the final shape produced by a given geometry mask is well solved, the reverse is not true. The inverse problem is defined as the determination of the mask and etching parameters that will shape the desired structure. We aim to address the inverse problem using non-convex optimization techniques.

The overall procedure employed to address this problem is illustrated in Figure 3. Essentially, it is an iterative process that refines the geometry of an etching mask.That the concept involves acquiring the mask required to produce a specific device through wet silicon etching, which serves as a cost-effective alternative for MEMS device fabrication but is non-trivial.

Owing to silicon's anisotropy, the masks produce structures that diverge from the patterns they depict. Consequently, comprehending how to attain a specific device utilizing this anisotropic etching technique could offer time and cost savings for manufacturers, as simulations would yield the desired outcomes.

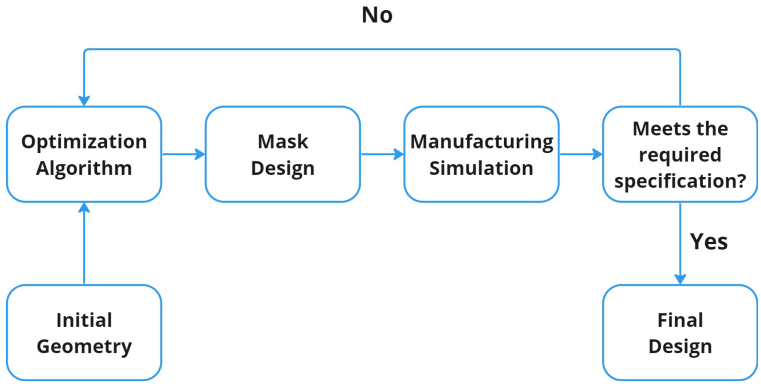

Figure 3: Mask optimization procedure.

In general, this algorithm involves codes in Python and C++, the structure of a simple genetic algorithm, and open-source software such as OpenSCAD and ViennaLS. It begins by determining the discretization of the ideal device in 3D. For this, the top view of the device is used, considering only two dimensions, since the mask obtained later in the genetic algorithm will use these 2D dimensions. The third dimension of the device will be achieved through etching and the analysis of etching time, which will be addressed later.

When discretizing your mesh, for example, if your device measures $10\mu m$ in width by $10\mu m$ in length, you could discretize it into 4 units of $5\mu m$ x $5\mu m$, or into 25 units of $2\mu m$ x $2\mu m$, or into 100 units of $1\mu m$ x $1\mu m$, as illustrated in Figure 4, panels a, b, and c, respectively.

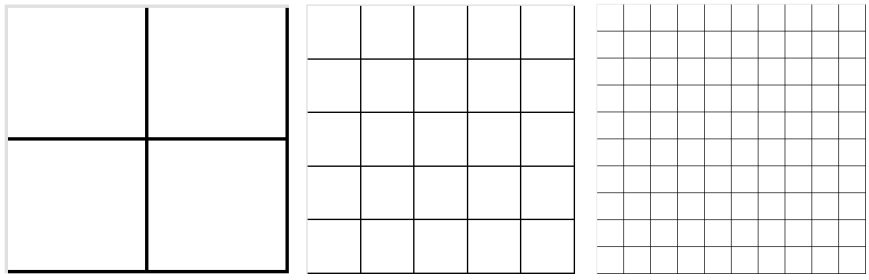

Figure 4: Discretization sizes.

In the genetic algorithm, discretization refers to the size of an individual, that is, the number of genes that the individual will have. Thus, the chosen discretization directly impacts the resolution of the problem. For instance, a very coarse resolution, such as 4 units of $5\mu m$ x $5\mu m$ in the example above, might result in insufficient definition of smaller structures or even their disappearance in the final device. Conversely, selecting a very fine discretization, such as 100 units of $1\mu m$ x $1\mu m$, may lead to prolonged computation times for reaching a final result. Therefore, for each device to be simulated, an individual analysis should be conducted to determine the appropriate level of discretization.

The individuals have a size determined by the discretization, but the genes can take values of 1 or 0. Points classified as 0 indicate that there is no mask at that point, meaning this area will be etched during the anisotropic simulation. Points classified as 1 indicate that there is material in the mask at that point, and therefore, no etching will occur at that location.

Since there are no existing works related to this approach, various tests with different discretizations were conducted, leading to the establishment of certain criteria for the algorithm, particularly regarding the genetic algorithm. Among these criteria are an initial population of 150 individuals and subsequent populations of 32 individuals, considering that an initial population is essential for maintaining genetic diversity. Additional details needed for forming subsequent populations will be addressed later. Furthermore, it was decided that the top 8 individuals would be selected for crossover and mutation stages to form the next generation.

Three types of crossover were performed with the 8 selected individuals. The first crossover, called single-point crossover, is simple and quick, involving a single segment exchange between parents. A random point is chosen, and genes up to this point are copied from the first parent, while genes after this point are taken from the second parent to generate a new individual.

The second crossover is the two-point crossover, where two points along the parents genes are chosen randomly. The genes between these two points are copied from the second parent, while the genes outside these points are copied from the first parent. Finally, the third crossover is the uniform crossover, where each gene is randomly chosen from either parent. Figure 5 shows an example of the three crossovers used. The latter two crossovers provide greater gene mixing with two exchange areas, thereby increasing genetic diversity.

In genetic algorithms, mutation is an operation that introduces genetic diversity into the population, helping to explore the solution space and preventing premature convergence to local optima. Mutation occurs directly in the 8 selected individuals and changes over generations. This is based on a percentage of the fitness values. As the values approach the desired criterion, the number of points undergoing mutation gradually decreases. If the fitness value of an individual is less than 1% of the volume of the ideal device, only one point is changed

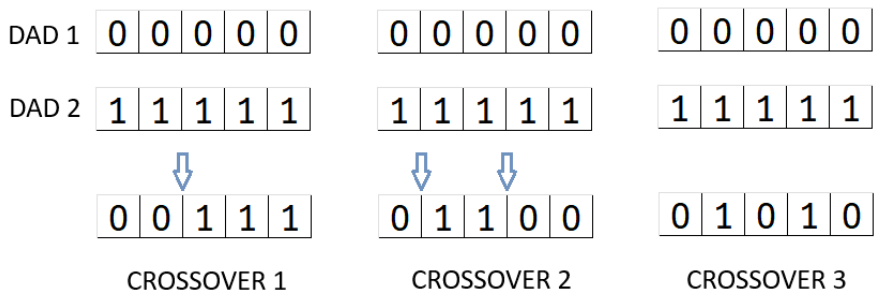

Figure 5: Crossover procedure.

by mutation. If it is greater than 1% and less than 2.5%, 2.5% of the total points (considering the total genes of an individual, or the mesh size) are altered. If it is greater than 2.5% and less than 5%, 5% of the total points are altered; and for values greater than 5%, 10% of the total points are altered by mutation.

Given that there are multiple generations with 32 individuals each, if each corrosion simulation process took a long time (for example, 10 minutes), the final algorithm would take days to achieve the desired result. Additionally, the etching rates in the main directions of the silicon substrate need to be defined for the simulation. In this work, we used the rates presented by [13], which are shown in Table 1.

Direction	Etch Rate $[\mu m/min]$
100	0.797
110	1.455
111	0.005
311	1.436

Table 1: Etch rates values.

Based on these rates and some simulations, Table 2 was created and using the values from Table 1 and the Equation 1 was constructed through linear regression, resulting in an r^2 value of 1, the r^2(coefficient of determination) in a linear regression is a statistical measure that represents the proportion of the variance in the dependent variable that is explained by the independent variables in the model. In other words, r^2 indicates how well the data fit the regression model.

$$z = 0,2116.t - 0,959 \tag{1}$$

This equation demonstrates the relationship between etching time (t) and depth (z). Hence, it is imperative to examine the deepest section of the structure for which the mask needs to be determined, allowing for the calculation of time in the algorithm.

The fitness value is the average volume of two structures derived from operations on the 3D structures. The first operation calculates the difference between the ideal 3D device and the test device (the one obtained from each individual mask) also in 3D. The second operation is the inverse, calculating the difference between

Time $[min]$	Depth $[\mu m]$
10	1.16
15	2.21
20	3.28
25	4.33
30	5.38
35	6.45
40	7.52
45	8.56
50	9.62

Table 2: Depth values.

the test device in 3D and the ideal device in 3D. This operation is performed using OpenSCAD software, and subsequently, the volume of each structure resulting from this operation is calculated using the VTK library in Python.

Figure 6illustrates the resulting structures obtained after the Boolean operations performed in OpenSCAD, which are used in the fitness evaluation process. The structure on the left represents the volume difference between the ideal 3D device and the test device, while the structure on the right shows the inverse, the volume difference between the test device and the ideal 3D model. The final fitness value is computed as the average volume of both resulting structures.

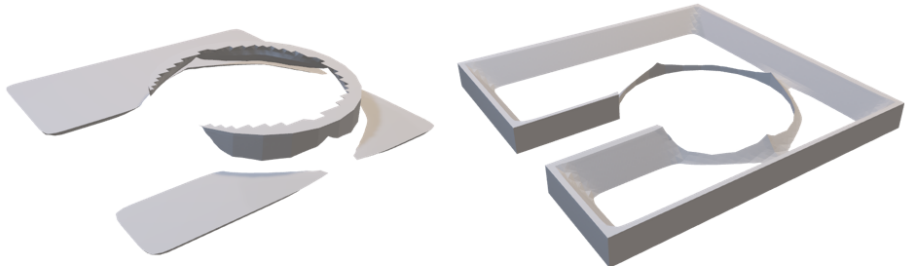

Figure 6: Structures after Boolean operations.

Finally, to determine the stopping criterion for the algorithm, we need to set a maximum value for this fitness. In this model if the average is less than 0.1% of the total volume of the desired device, we can consider that the solution to the problem has been found.

The final volume percentage that defines the stopping criterion can be adjusted and is set to a specific threshold for each structure. Although the mesh could still be further refined, the results are already visually satisfactory in terms of structural shape. In this work, the ideal model was simulated using a program that considers the crystalline structure of silicon. Therefore, the acceptable volume difference threshold had to be reduced until convergence between the structures was achieved. In contrast, for models designed using conventional 3D modeling software - which do not account for crystal structures - a higher volume percentage can be tolerated.

Figure 7 illustrates more clearly how decreasing the maximum allowed volume percentage in the algorithm's stopping criterion leads to the desired structure, as shown in Fig. 8, which was created using standard modeling tools.

Figure 7: Structures after Boolean operations.

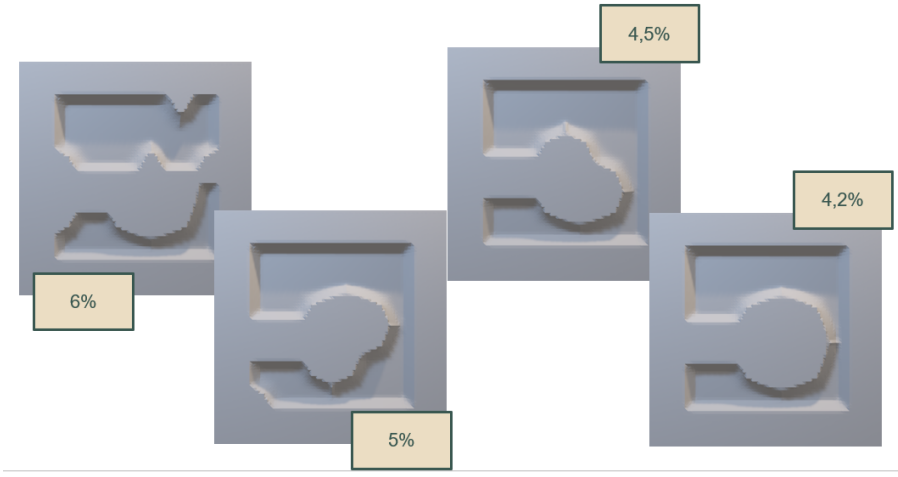

Figure 8: Resulting beams for each stopping criterion.

All values are displayed in Table 3. In addition to the variables in this table, the user must also:

- Discretize the structure of the device.
- Determine the etching time.
- Insert the volume of the ideal device.

The overall structure of the algorithm is depicted in Figure 9. An initial random population is formed, based on the number of points determined by the discretization of the structure. Manufacturing simulation is performed using ViennaLS, followed by a comparison analysis between these structures with openScad and measured with python VTK.

Item	Value
Chromosome array length	Determined by discretization
Initial population size	150 individuals
Subsequent populations size	32 individuals
Selected individuals	8
Crossover types	3
Mutation	Percentage of genes
Corrosion time	15 minutes
Stop criteria	0.1% of ideal volume
Max generations	1000

Table 3: Algorithm values,

So, if this comparison yields a result below the stop criteria (0.1% of ideal volume, the s), the final structure is very similar to the desired one, and therefore, the mask that produces it can be found. If it is greater, the structures that are more similar are selected to undergo crossover and mutation processes between them, generating a new population, and the process of fitness calculation is restarted.

To conclude the methodology, in addition to the primary approach where the user can either input the etching time manually into the algorithm or iteratively conduct experiments to converge on an optimal time starting from the value suggested by Equation 1 an advanced algorithm was developed to autonomously adjust the etching time as the fitness values stabilize. Given the inherent uncertainties of the fabrication process, this automated method is particularly advantageous, as it allows simultaneous exploration of etching time, mask design, and process conditions. This not only mitigates the reliance on costly, time consuming experiments but also provides substantial efficiency gains for industrial applications.

During the execution of the genetic algorithm, the previously fixed etching time becomes dynamic, re-assessed at each iteration. The algorithm bases its adjustments on the average fitness values of the top eight individuals over the preceding five generations. This average, initially computed using the volume of the initial device, is continuously recalculated as new generations evolve, creating a moving average of averages. Thus, the metric used for analysis is the mean of the mean fitness values from the last five generations, offering a more comprehensive insight into the system's convergence.

In cases where uncertainty arises, it is advisable to initiate the algorithm with an etching time slightly below the value estimated in Equation 1. The algorithm monitors the moving averages, and if it detects a stabilization where the difference between the current generation's average and the average of the last five generations is within 3% the etching time is incremented by 1 minute. Conversely, if the average fitness begins to increase, signaling that the etching time has exceeded the optimal duration, the algorithm reduces the time accordingly. Once this adjustment is made, the process continues with the new time until final convergence is achieved.

4 SIMULATION AND RESULTS

First, tests were conducted in triplicate for three distinct structures, one in the island model and two in the beam model but with different shapes, with the same discretization but different sizes of structure. These three structures were initially selected because they are commonly observed in anisotropic wet etching of silicon, as shown in the works of [9], [15] and [2].

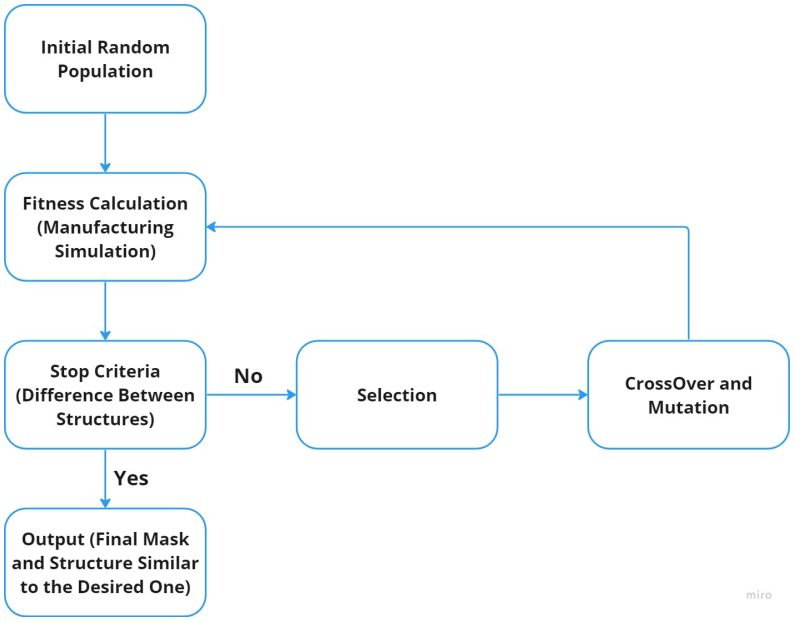

Figure 9: Genetic algorithm procedure.

Each of the structures has a different size, but all were discretized at $5\mu m$ and a etching time of 15 minutes. Table 7 provides detailed information on the dimensions of each structure, the discretization, the number of points into which it was subdivided (size of the individual in the genetic algorithm), and the time taken by the genetic algorithm to obtain the solution, i.e., to derive the mask that produces these structures in an anisotropic wet etching of silicon and Figure 10 shows these structures.

Structure $[\mu m^2]$	Dimension $[\mu m]$	Discretization points	Number of generations	Number of $[min]$	Time
Island	20 x 20	5	16	4	105
Beam 1	30 x 30	5	36	21	145
Beam 2	30 x 40	5	48	32	199

Table 4: First test results.

To gain a deeper insight into the disparity between the final structures post-etching and the masks utilized in the photolithography phase, Figure 11 illustrates the initial tested structure, namely the island model. The left-hand side depicts the mask image, while the right-hand side showcases the ultimate structure following the corrosion process. Similarly, the other two beam structures are displayed in Figures 12 and 13.

To further assess the algorithm's performance, the island and the initial beam structures were reprocessed under identical conditions, both resized to $30\mu m$ x $30\mu m$, with the etching time fixed at 20 minutes. The algorithm required 17 generations and 240 minutes to converge on a solution for the island, whereas for the beam, it took 19 generations and 316 minutes. Figure 14 illustrates the fitness values for the island structure

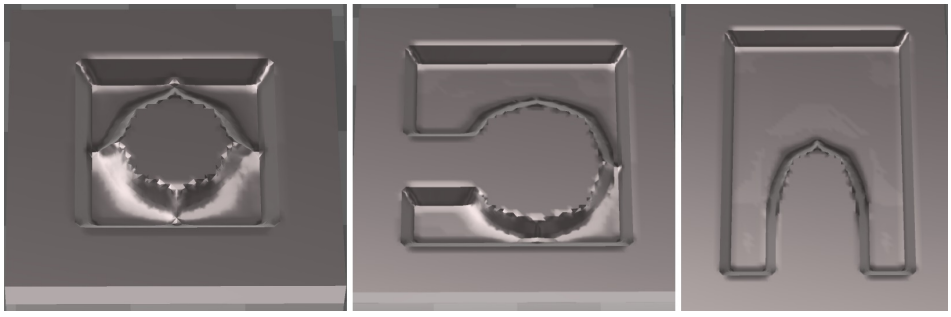

Figure 10: Three desired etched structures.

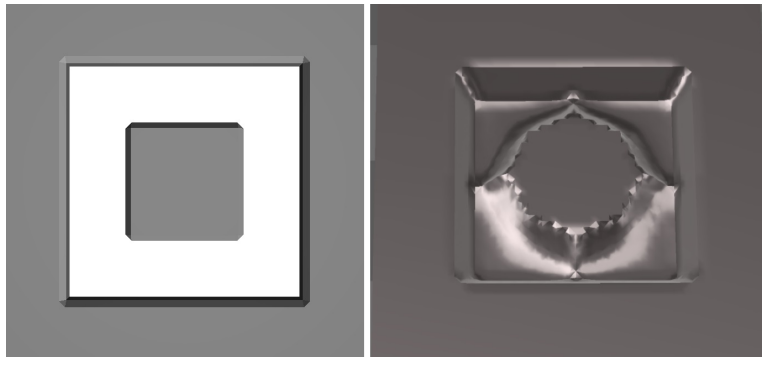

Figure 11: Island mask and structure.

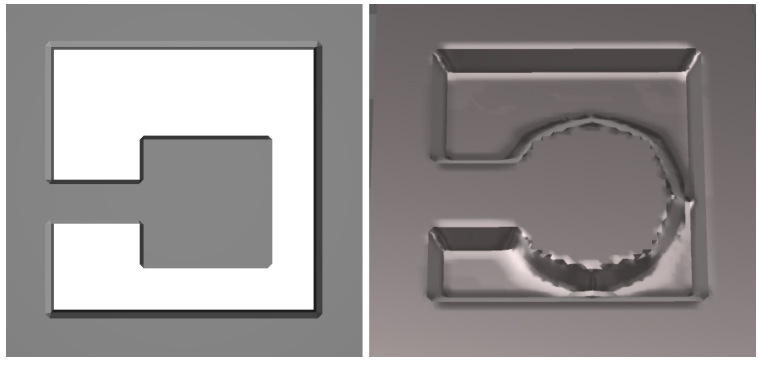

Figure 12: Beam mask and structure.

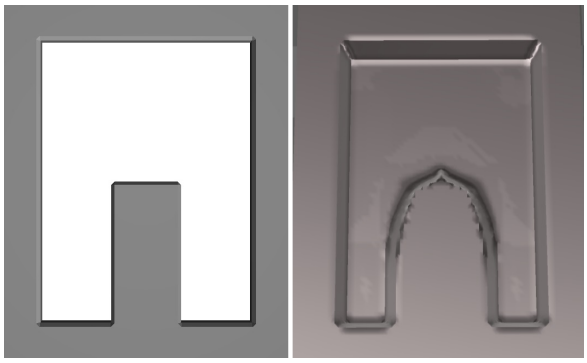

Figure 13: Beam 2 mask and structure.

throughout the algorithm's execution, with the blue line representing the mean fitness values of each generation and the orange line indicating the minimum fitness values per generation. Similarly, Figure 15 presents the corresponding data for the beam structure, following the same schema.

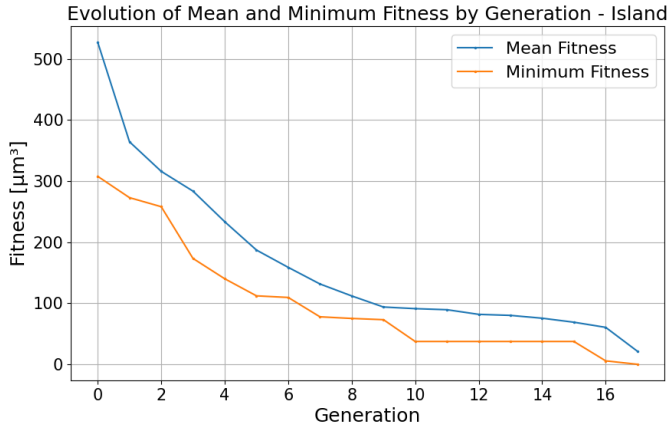

Figure 14: Proposed genetic algorithm evolution island.

Analysis of the graphs reveals the convergence behavior of the algorithm and the impact of mutations on the final values. It is evident that the minimum values for each generation differ somewhat from the mean values, reflecting the influence of mutation on the algorithm's performance.

It is crucial to acknowledge that the number of generations can vary significantly due to the stochastic nature of this genetic algorithm, where the initial population, crossover, and mutation processes are randomized. Despite this variability, the results remain consistent, as demonstrated by the convergence patterns observed across the algorithm's generations and iterations in the graphs.

Focusing now on optimized MEMS gyroscopes, [16] presents the design, fabrication, and characterization of a novel high-quality resonant gyroscope for tilt/roll measurement, implemented on a 40 μm (100) silicon-on-insulator (SOI) substrate without using the deep reactive ion etching (DRIE) process. [16] also emphasize that the elimination of deep reactive ion etching (DRIE) of silicon in the anisotropically wet-etched gyroscope

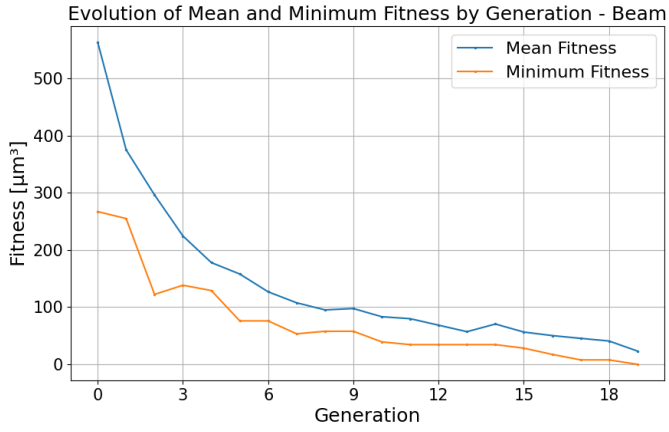

Figure 15: Proposed genetic algorithm evolution beam.

improves the robustness of the gyroscope against process variation and reduces manufacturing costs.

Figure 16 shows the ideal gyroscope, fabricated using anisotropic wet etching of silicon. The proposed algorithm in this work was used to propose a mask for a similar device. One strategy employed is to subdivide its final structure into smaller structures so that the algorithm reaches solutions more quickly. In this case, the device was subdivided, and Figure 17 shows the structure to be found alongside the mask and the final structure identified by the algorithm.

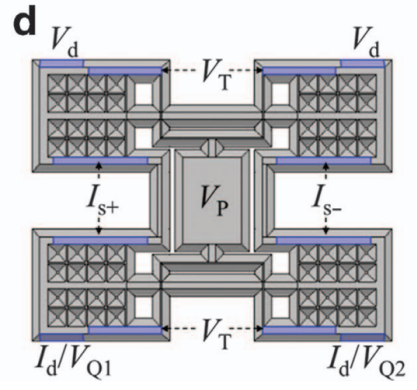

Figure 16: Optimized gyroscope [16].

In addition to the standard approach, where the etching time is either manually input by the user or determined through experimentation, a second algorithm was developed to automatically adjust the etching time based on the stabilization of fitness values. This method optimizes the silicon etching process, particularly when the etching behavior is not well understood, offering a more efficient alternative.

The proposed algorithm monitors convergence by tracking the mean fitness of the top eight individuals in each generation. Specifically, it computes the average fitness of the best eight individuals per generation and, starting from the sixth generation, calculates a moving average over the most recent five generations. This

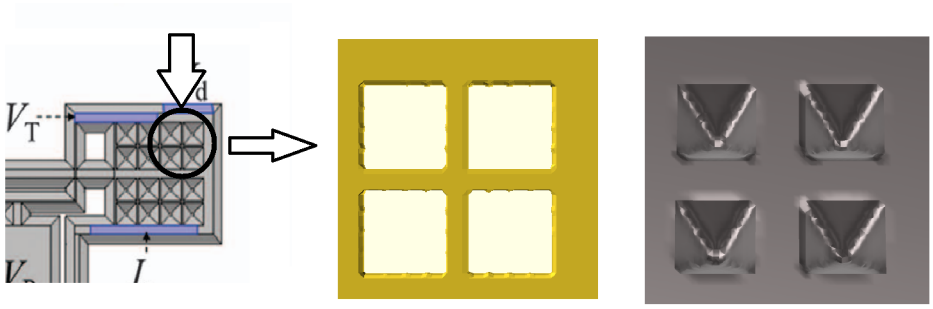

Figure 17: Optimized gyroscope mask and structure.

rolling average serves as the primary metric to guide dynamic adjustments to the etching time.

The optimization process begins with an initial time estimate derived from Equation 1. At each iteration, the algorithm compares the current five-generation average with the previous one (e.g., generations 1 to 5 compared to 2 to 6, then 2 to 6 to 3 to 7, etc.). If the difference between consecutive five-generation averages falls below a 3% threshold, this is interpreted as an indication of convergence, and the etching time is incremented by one minute.

If the observed average fitness begins to increase, this is interpreted as a signal that the etching time has surpassed the optimal point. In such cases, the algorithm decreases the etching time and continues iterating toward convergence. This adaptive strategy significantly enhances the efficiency of the optimization process by minimizing reliance on exhaustive experimental iterations, thereby reducing both the time and cost associated with physical validation.

However, this approach becomes somewhat more complex. Using the algorithm that proposes this etching time for the two examples above, it was possible to obtain a satisfactory result with the algorithm converging to the desired structure. Table 5 shows the time for complete execution until the algorithm converged for both situations.

Model	Dimension $[\mu m^2]$	Discretization $[\mu m]$	Number of points	Number of generations	Time $[min]$
Island	30 x 30	5	36	17	176
Beam	30 x 30	5	36	23	218

Table 5: Results algorithm time - island x beam.

This algorithm performed well for structures with 36 genes per individual, as shown in Figures 18 and 19, which display the average fitness values of each generation (blue line), the minimum fitness values per generation (orange line), and the points where there is an automatic change in the etching time suggested by the algorithm. It is possible to observe a stagnation in the generations prior to the time change in both situations. In the case of the island, the change was made at the end of generation 16, and in the case of the beam, at the end of generation 12, with the altered time starting in the following generation.

In both cases, the algorithm reached the correct etching time, determined to be 20 minutes, with a volume difference of less than 0.1% from the ideal device volume, resulting in the correct final convergence of the algorithm. Considering the automatic increment of the etching time, although it yields good results for smaller

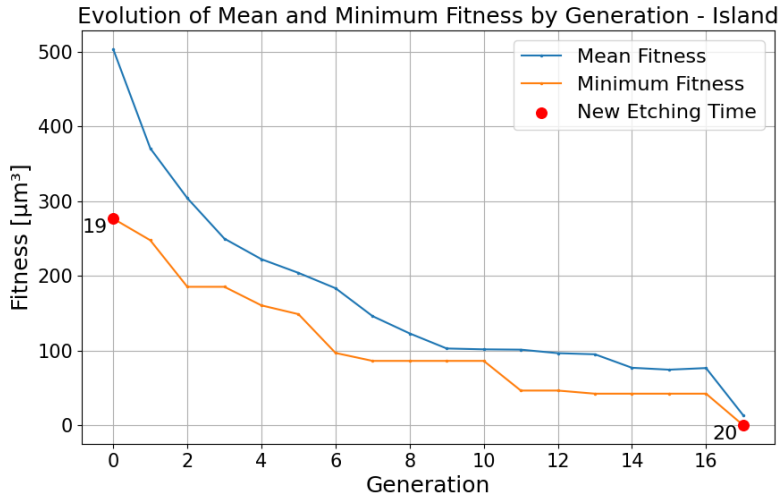

Figure 18: Proposed genetic algorithm evolution with time island.

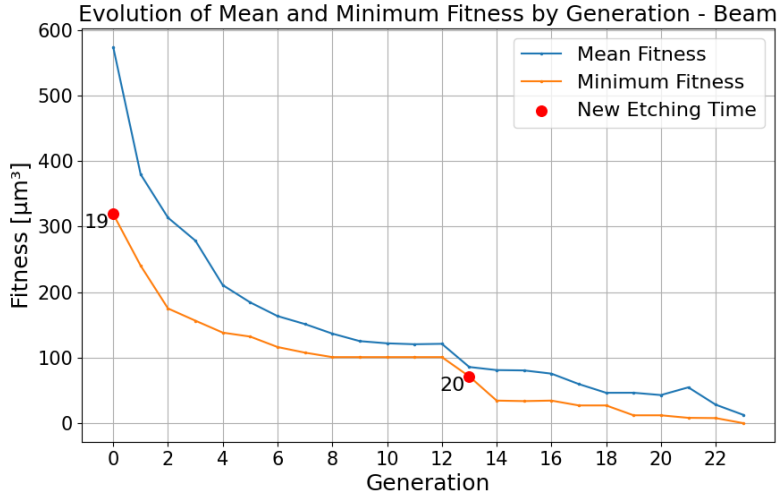

Figure 19: Proposed genetic algorithm evolution with time beam.

structures, such as the above case with 36 genes, the algorithm takes much longer to solve larger problems, like the previously mentioned gyroscope example, where individuals contain 100 genes.

A point to highlight in the case of this optimized gyroscope is that all the etched structures are identical and have a final meeting point between the silicon's crystalline orientation lines, which precisely form these inverted pyramids. In this case, the automatic time evaluation by the algorithm may not be accurate, as even if the etching time increases, there will be no change in the final etched depth once it stagnates at this depth point. Therefore, it is important to emphasize that each case should be individually evaluated to select the best approach. As this is a completely new approach in the literature, several new steps should be explored in the future to optimize this algorithm.

5 CONCLUSION

In light of the images of the structures, it becomes apparent that the formations are non-trivial, particularly exhibiting differences at directional changes or "corners". Considering a scenario where the manufacturing of these devices is widespread, this study represents a groundbreaking approach to the production of MEMS devices, using wet corrosion and anisotropy to achieve the desired structures.

The innovation of this work is underscored by the lack of similar studies in the current literature, which results in significant challenges in evaluating the variables used. The absence of prior work with this approach precludes direct comparison of the obtained results. However, considering the structures that the algorithm was able to achieve and the stopping criterion, a volume difference of less than 0.1%, it can be considered that the objective has been successfully met.

The convergence within few generations can be attributed to the relationship between the number of generations and the discretization level of the initial structure, as well as the initial guess for the etching time. When the structure is represented with a lower number of points and the initial time estimate is close to the optimal value, the algorithm reaches convergence more rapidly. Furthermore, through experimental testing, it was observed that increasing the number of individuals in the initial population, set at 150 in this case, contributed to accelerating the convergence process.

In a scenario where the manufacturing of these devices is widespread, this study could signify the beginning of a novel approach for producing MEMS devices using wet corrosion and leveraging anisotropy to achieve the desired structure. However, there are still aspects that could be integrated into the process to ensure the adaptability of this algorithm to various types of problems.

6 NEXT STEPS

For the next steps, efforts will focus on enhancing the algorithm's efficiency, particularly by incorporating time iterations directly into the genetic algorithm. This adjustment aims to allow for the use of more robust structures, optimizing the algorithm's performance in generating effective solutions. Additionally, further refinement will involve using finer discretization, enabling the derivation of non-rectangular mask shapes, and supporting the development of larger final devices, such as accelerometers and gyroscopes.

ACKNOWLEDGEMENTS

This research is a part of the PDIP FAPESP. The authors thank PPGEM-USP and FAPESP for financial support to the development of this project under Grant Agreement No. 2019/18818-6.

ORCID

Ana Paula Rehder, http://orcid.org/0000-0001-8836-7058

Marcos Sales Guerra Tsuzuki, http://orcid.org/0000-0002-8495-2337
Thiago de Castro Martins, http://orcid.org/0000-0003-1692-3849

REFERENCES

[1] Bean, K.: Anisotropic etching of silicon. IEEE Transactions on Electron Devices, 25(10), 1185–1193, 1978. http://doi.org/10.1109/t-ed.1978.19250.

[2] Fang, J.; Wang, X.; Hu, C.; Lv, Z.; Shi, S.; Yuan, J.; Liu, S.; Gao, C.: Research of wet etching in hf-based solution to release soi-based gyroscope micro-structures. In 2013 14th International Conference on Electronic Packaging Technology, 671–675. IEEE, 2013.

[3] Gibbs, M.S.; Maier, H.R.; and, G.C.D.: Relationship between problem characteristics and the optimal number of genetic algorithm generations. Engineering Optimization, 43(4), 349–376, 2011. http://doi.org/10.1080/0305215X.2010.491547.

[4] Goldberg, D.E.: Genetic Algorithms in Search, Optimization and Machine Learning. Addison-Wesley Longman Publishing Co., Inc., USA, 1st ed., 1989. ISBN 0201157675.

[5] Holland, J.H.: Adaptation in natural and artificial systems: an introductory analysis with applications to biology, control, and artificial intelligence. MIT press, 1992.

[6] Maluf, N.; Williams, K.: Introduction to microelectromechanical systems engineering. Artech House, Boston, 2004. ISBN 1-58053-590-9.

[7] Nascimento, L.B.P.; dos Santos, V.G.; da Silva Pereira, D.; Aranibar, D.B.; Patino-Escarcina, R.E.; de Morais, D.S.; de Andrade Pimentel, V.C.; Alsina, P.: Uma abordagem baseada em algoritmo genetico para a suavizacao de caminhos para espuma probabilistica. Anais do 14o Simposio Brasileiro de Automacao Inteligente, 2019.

[8] Osher, S.; Fedkiw, R.; Piechor, K.: Level set methods and dynamic implicit surfaces. Appl. Mech. Rev., 57(3), B15–B15, 2004. http://doi.org/10.1115/1.1760520.

[9] Pal, P.; Sato, K.: Fabrication methods based on wet etching process for the realization of silicon mems structures with new shapes. Microsystem technologies, 16, 1165–1174, 2010.

[10] Pal, P.; Swarnalatha, V.; Rao, A.V.N.; Pandey, A.K.; Tanaka, H.; Sato, K.: High speed silicon wet anisotropic etching for applications in bulk micromachining: a review. Micro and Nano Systems Letters, 9(1), 4, 2021. http://doi.org/10.1186/s40486-021-00129-0.

[11] Partnership, P.F.: An Introduction to MEMS (Micro-electromechanical Systems). PRIME Faraday Partnership, Stevenage, 2002. ISBN 1-84402-020-7.

[12] Radjenović, B.; Radmilović-Radjenović, M.: 3D simulations of the profile evolution during anisotropic wet etching of silicon. Thin Solid Films, 517(14), 4233–4237, 2009.

[13] Radjenović, B.; Radmilović-Radjenović, M.; Mitrić, M.: Level set approach to anisotropic wet etching of silicon. Sensors, 10(5), 4950–4967, 2010. http://doi.org/10.3390/s100504950.

[14] Seidel, H.; Csepregi, L.; Heuberger, A.; Baumgaertel, H.: Anisotropic etching of crystalline silicon in alkaline solutions. ii. influence of dopants. Journal of the Electrochemical Society, 137, 3626–3632, 1990.

[15] Wang, X.; Xu, X.b.; Zhang, D.w.; Wu, X.z.: Pre-buried mask wet etching for suspended silicon microstructures applied in rocking mass micro-gyroscope. Microsystem Technologies, 24, 1081–1087, 2018.

[16] Wen, H.; Daruwalla, A.; Ayazi, F.: Resonant pitch and roll silicon gyroscopes with sub-micron-gap slanted electrodes: Breaking the barrier toward high-performance monolithic inertial measurement units. Microsystems & nanoengineering, 3(1), 1–9, 2017.

[17] Whitaker, R.T.: A level-set approach to 3d reconstruction from range data. International Journal of Computer Vision, 29(3), 203–231, 1998. http://doi.org/10.1023/a:1008036829907.